

chains that could be derivatized, it should be possible to tune their properties for applications such as vehicles for drug and biomolecule delivery, cages for trapping functional enzyme cascades that allow flux of starting materials and products, components of sensing systems, and new frameworks for the development of protocells (24).

References and Notes

- H. F. Lodish, *Molecular Cell Biology* (W.H. Freeman, New York, ed. 6, 2008).
- S. Tanaka *et al.*, *Science* **319**, 1083 (2008).
- C. M. Agapakis, P. M. Boyle, P. A. Silver, *Nat. Chem. Biol.* **8**, 527 (2012).
- D. A. Hammer, N. P. Kamat, *FEBS Lett.* **586**, 2882 (2012).
- M. Uchida *et al.*, *Adv. Mater.* **19**, 1025 (2007).
- R. M. Capito, H. S. Azevedo, Y. S. Velichko, A. Mata, S. I. Stupp, *Science* **319**, 1812 (2008).
- F. Boato *et al.*, *Angew. Chem. Int. Ed. Engl.* **46**, 9015 (2007).
- S. Raman, G. Machaidze, A. Lustig, U. Aebi, P. Burkhard, *Nanomedicine* **2**, 95 (2006).
- N. P. King *et al.*, *Science* **336**, 1171 (2012).
- Y. T. Lai, D. Cascio, T. O. Yeates, *Science* **336**, 1129 (2012).
- B. Wörsdörfer, K. J. Woycechowsky, D. Hilvert, *Science* **331**, 589 (2011).
- J. C. Sinclair, K. M. Davies, C. Vénien-Bryan, M. E. M. Noble, *Nat. Nanotechnol.* **6**, 558 (2011).
- J. D. Brodin *et al.*, *Nat. Chem.* **4**, 375 (2012).
- M. M. Pires, J. Lee, D. Ernenwein, J. Chmielewski, *Langmuir* **28**, 1993 (2012).
- E. H. C. Bromley, K. Channon, E. Moutevelis, D. N. Woolfson, *ACS Chem. Biol.* **3**, 38 (2008).
- A. N. Lupas, M. Gruber, *Adv. Protein Chem.* **70**, 37 (2005).
- D. N. Woolfson, *Adv. Protein Chem.* **70**, 79 (2005).
- J. M. Fletcher *et al.*, *ACS Synth. Biol.* **1**, 240 (2012).
- E. H. C. Bromley, R. B. Sessions, A. R. Thomson, D. N. Woolfson, *J. Am. Chem. Soc.* **131**, 928 (2009).
- Materials and methods are available as supplementary materials on *Science* Online.
- R. L. Harniman *et al.*, *Nanotechnology* **23**, 085703 (2012).
- www.quorumtech.com/pdf/SputterCoatingTechniques/Sputter_coating_technical_brief.pdf
- G. Offer, R. Sessions, *J. Mol. Biol.* **249**, 967 (1995).
- S. S. Mansy *et al.*, *Nature* **454**, 122 (2008).
- E. K. O'Shea, R. Rutkowski, P. S. Kim, *Science* **243**, 538 (1989).

Acknowledgments: We thank the Woolfson group for valuable discussions; the BBSRC for funding to D.N.W. and P.J.B. (BB/G008833/1) and for a studentship to A.L.B.; and the EPSRC for studentships to R.L.H. and T.H.S. J.M. is supported by a Wellcome University Award. We are grateful to the University of Bristol Advanced Computing Research Centre and the eInfrastuctureSouth Consortium for high-performance computing; and Jonathan Jones and the EM Unit (EMU) School of Chemistry University of Bristol for EM access. The peptides described have been added to the Pcomp database for synthetic biology (<http://coiledcoils.chm.bris.ac.uk/pcomp/index.php>).

Supplementary Materials

www.sciencemag.org/cgi/content/full/science.1233936/DC1
Materials and Methods
Figs. S1 to S15
Tables S1 to S3
References (26–38)
Movie S1

11 December 2012; accepted 11 March 2013
Published online 11 April 2013;
10.1126/science.1233936

Amplifying Genetic Logic Gates

Jerome Bonnet, Peter Yin,* Monica E. Ortiz, Pakpoom Subsoontorn, Drew Endy†

Organisms must process information encoded via developmental and environmental signals to survive and reproduce. Researchers have also engineered synthetic genetic logic to realize simpler, independent control of biological processes. We developed a three-terminal device architecture, termed the transcriptor, that uses bacteriophage serine integrases to control the flow of RNA polymerase along DNA. Integrase-mediated inversion or deletion of DNA encoding transcription terminators or a promoter modulates transcription rates. We realized permanent amplifying AND, NAND, OR, XOR, NOR, and XNOR gates actuated across common control signal ranges and sequential logic supporting autonomous cell-cell communication of DNA encoding distinct logic-gate states. The single-layer digital logic architecture developed here enables engineering of amplifying logic gates to control transcription rates within and across diverse organisms.

Researchers have used genetically encoded logic, data storage, and cell-cell communication to study and reprogram living systems, explore biomolecular computing, and improve cellular therapeutics (1–9). Most approaches to engineering cell-based logic champion two-terminal device architectures upon which gate-gate layering, similar to conventional electronics, is used to realize all logic functions (10, 11). Despite recent advances (11, 12), such designs are difficult to scale because of problems associated with reusing regulatory molecules within the self-mixing environments of individual cells. As representative examples, a single-cell two-input “exclusive or” (XOR) gate, a function whose output is high only if the inputs are different, required controlled expression of four gate-specific regulatory molecules from four plasmids (12); an amplifying “exclusive nor” (XNOR) gate, high output only if inputs are equal, has not been demonstrated within single cells (10).

We instead sought a device architecture in which the same regulatory molecules could be simply reused to implement all logic gates within a single logic layer (13). We also sought to decouple the signals controlling gate switching from gate inputs and outputs. Realizing both goals would enable straightforward engineering of distinct gates with constant switching thresholds and support signal gain and amplification if desired. Lastly, we wanted all gate signals to be encoded via a common signal carrier supporting connectivity within natural systems and across a diverse family of engineered genetic devices (14).

We combined earlier concepts (14–17) to invent a transistor-like three terminal device (18) termed the transcriptor. Independent control signals govern transcriptor logic elements that regulate transcriptional “current,” defined by the flow of RNA polymerase along DNA (Fig. 1A). Gate input and output signals are transcription rates at positions on DNA marking logic element boundaries. Logic elements use asymmetric transcription terminators as reversible check valves that disrupt RNA polymerase flow in only one of two possible orientations (Fig. 1B). Recombinases catalyze unidirectional inversion of DNA within

opposing recognition sites (Fig. 1B) or deletion of DNA between aligned sites (Fig. 1C), providing independent control over the orientation or presence of one or more terminators. Stated differently, we developed a device architecture similar to a transistor but leveraged unique properties of genetic regulation to implement all gates without requiring that multiple instances of simpler gates be connected in series (i.e., without layering) (18, 19).

For example, a transcriptor XOR logic element requires bracketing one asymmetric transcription terminator with two pairs of opposing recombination sites recognized by independent integrases (Fig. 1D). If neither integrase is expressed, then the terminator blocks transcription (Fig. 1D, top). Expression of either integrase alone inverts the DNA encoding the terminator and allows transcription to flow through the transcriptor (Fig. 1D, middle). Expression of both integrases inverts and then restores the original orientation of the terminator, again blocking transcription (Fig. 1D, bottom). A complete XOR gate requires placing an XOR logic element within a three-terminal device in which integrase expression is controlled by two independent control signals (Fig. 1E).

We designed additional transcriptor logic elements encoding Boolean OR, NOR, XNOR, and AND functions for use within a common gate architecture (Fig. 2 and fig. S1). Straightforward changes only to logic element DNA were sufficient to design functionally distinct gates expected to be responsive to identical control signals. Designing a transcriptor-only “not and” (NAND) element, low output only if both control signals are high, proved more challenging. We instead used a hybrid architecture that combines flipping of a terminator along with a constitutive promoter. Although noncanonical, the NAND gate still responds to the same control signals while exhibiting varied output levels (below).

Department of Bioengineering, Y2E2-269B, 473 Via Ortega, Stanford, CA 94305-4201, USA.

*Present address: Department of Biology, University of Pennsylvania, Philadelphia, PA 19104, USA.

†Corresponding author. E-mail: endy@stanford.edu

Transcript elements allowing unidirectional processing of DNA produce permanent gates that implement write-once logic operations. However, recombination directionality factors (RDFs) can reverse DNA inversion by integrases (20). We designed rewritable transcript elements in which controlled expression of RDFs, given constitutive integrase expression, should implement reversible logic and demonstrated a reversible buffer gate controlled by a single RDF (figs. S2 and S3); reversible gates require the same number of regulated factors as permanent gates (e.g., two RDFs versus two integrases). Permanent gates are useful for applications requiring tracking or processing of historical signals (e.g., terminal differentiation during development or accumulated responses to asynchronous environmental cues), whereas reversible gates support multicycle computing (e.g., a synchronized cell division cycle counter).

We selected unidirectional serine integrases from bacteriophages TP901-1 and Bxb1 to control gate switching; these recombinases do not require host cofactors and have been shown to function in bacteria, fungi, plants, and animals (21). We recently implemented a rewritable digital latch by using the Bxb1 integrase and RDF to repeatedly flip a DNA memory element between two states (5); this class of latches are controlled by continuous transcription signals (i.e., analog inputs) that produce recombinase proteins sufficient to flip (or not) a DNA element (i.e., digital output) and thus can be abstracted and reused (22) as analog-to-digital converters.

We made a recombination control plasmid expressing the TP901-1 and Bxb1 integrases un-

der the control of exogenous arabinose (ara) and anhydrotetracycline (aTc) induction, respectively (23). We measured the propensities of TP901-1 and Bxb1 integrases to recognize and process specific DNA recombination sites (fig. S4A). We fitted abstracted Hill functions representing observed DNA processing propensities given increasing expression levels for each integrase alone (fig. S4B). We defined logic function models specific to each gate (fig. S4C) and predicted the expected behavior of multi-input gates directly from single-integrase Hill functions (Fig. 2).

We constructed low-copy plasmids encoding AND, OR, XOR, NAND, NOR, and XNOR logic elements between a standard strong prokaryotic promoter (input signal source) and green fluorescent protein (GFP) expression cassette (indirect output signal reporter) (23). We measured bulk GFP levels from bacterial cultures expressing varying amounts of TP901-1 and Bxb1 integrases controlling the six Boolean gates. Observed GFP expression patterns were well matched to predictions for all gates (Fig. 2); exact output levels varied among and within some gates (described below).

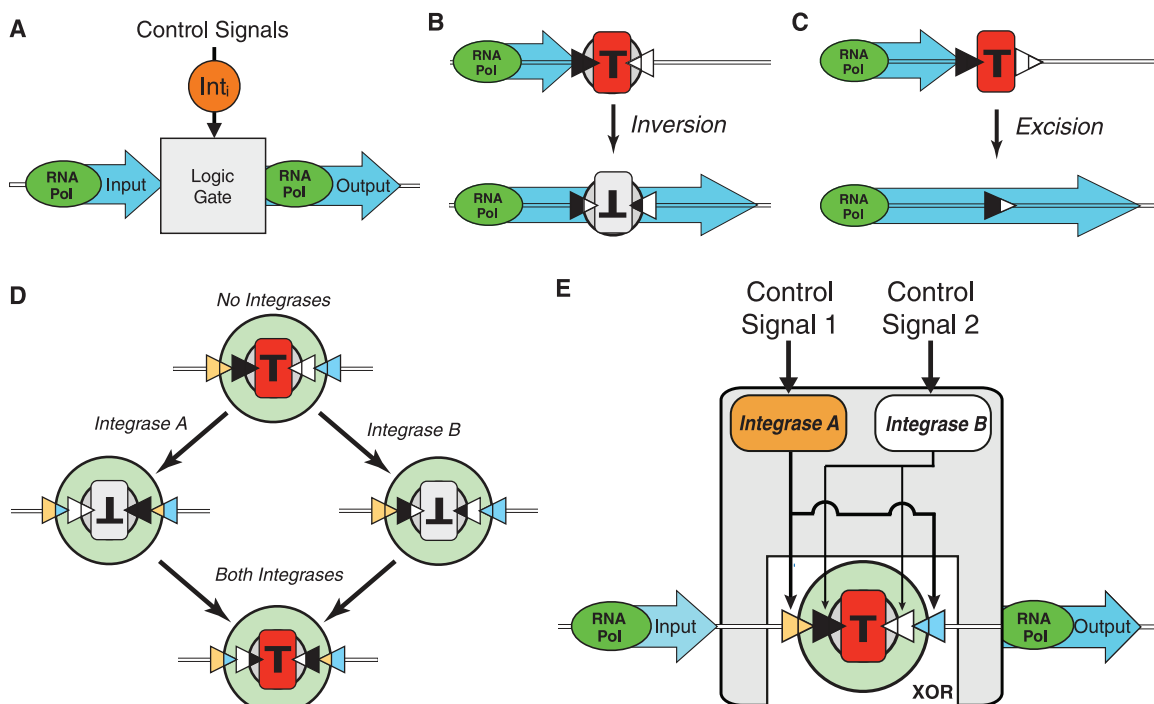
Transcript-based gates use discrete enzymatic processing of DNA to modulate RNA polymerase flow through logic elements. We thus expected that single cells might exhibit discontinuous (e.g., all or none) responses to small changes in control signals. For example, we measured fluorescence output distributions among single cells exposed to low or high control signals and found a single threshold defining distinct low/high outputs across all gates (Fig. 2, red

vertical line). To better study control signal digitization (i.e., the extent to which gate outputs are more digital than gate control signals across small changes in control signals), we compared changes in gate outputs to increasing control signals by using a common reporter (figs. S5 to S8). For example, we found that XOR gates switch completely between 0.2 and 2 ng/ml aTc and 0.0001 to 0.001% ara, whereas both control signals increase gradually across these inducer ranges (Fig. 3, A and B, and figs. S6 to S8). We defined a digitization error rate as the combined probability of scoring false high or low gate outputs in response to intermediate control signal changes, optimized thresholds for controllers and gates that best discriminate between putative low and high outputs, and quantified digitization error rates for each gate. AND, OR, XOR, and XNOR gates digitized aTc-induced control signals to varying degrees, whereas AND, OR, NOR, XOR, and XNOR gates digitized ara-induced signals (Fig. 3, C and D); no gates reduced digitization (Fig. 3, C and D), and all gates realized digital outputs in response to low/high control signals (Fig. 2).

Changes in gate outputs must be compared directly to changes in gate control signals to determine whether gates function as amplifiers (24, 25). We calculated population-average GFP levels for each control signal and gate outputs (fig. S5). We directly compared changes in gate outputs to the changes in gate control signals needed to activate gate switching, both for absolute (figs. S9 and S10) and normalized (Fig. 4) expression levels. We evaluated all gates across control-signal ranges needed to drive the least-

Fig. 1. Using transcriptors to implement three-terminal Boolean integrase logic gates.

(A) Three-terminal transcript-based gates use integrase (Int) control signals to modulate RNA polymerase (RNA Pol) flow between a separate gate input and output. **(B)** A canonical transcript element wherein an asymmetric transcription terminator (T) blocks transcriptional current in one orientation (red) or, when flipped, the opposite orientation (gray). Opposing recombination sites (black/white triangles) flank the terminator and direct flipping by an integrase. **(C)** Integrases can also excise DNA between aligned recombination sites. **(D)** State diagram for a transcript "exclusive or" (XOR) logic element: Opposing sites recognized by two independent integrases (blue/orange and black/white) are nested and flank one terminator. Recombination can produce four distinct states controlling terminator orientation. **(E)** The logic element from (D) within a three-terminal Boolean integrase XOR gate such that gate output is high only if control signals are different.



responsive gate (NAND) and did not normalize outputs via subtraction of lowest values, which otherwise greatly increases fold-change estimates. All gates generate increased absolute and fold-change differences in expressed output protein levels relative to those produced from the integrase controllers (Fig. 4 and figs. S9 and S10).

We confirmed that permanent transcription-based gates support sequential logic based on the heritable storage of logic element states in response to asynchronous control signals. For example, cells encoding AND and XNOR gates

were exposed to various patterns of integrase control signals, recording and generating appropriate outputs across ~40 cell doublings (fig. S11). Building from these results, we engineered cell-cell communication of DNA (7) encoding logic gates at different stages of gate activation (fig. S12), a feature unique to gates whose operation involves direct processing of DNA. We also assayed recombination response times, finding that 15-min control-signal pulses were sufficient to activate integrase-mediated switching (fig. S13 and movie S1).

During the course of responding to reviewer questions and preparing the final version of this manuscript, a system of two terminal logic gates was described by Siuti *et al.* based on flipping terminator, promoter, and gene elements (26). The family of Boolean integrase logic gates introduced here differs in the consistent use of a three-terminal device architecture that decouples logic-gate operation from both input and output signals, enabling simple tuning via changes to the transcription input signal (fig. S14) and ready reuse (e.g., reprogramming of natural transcription

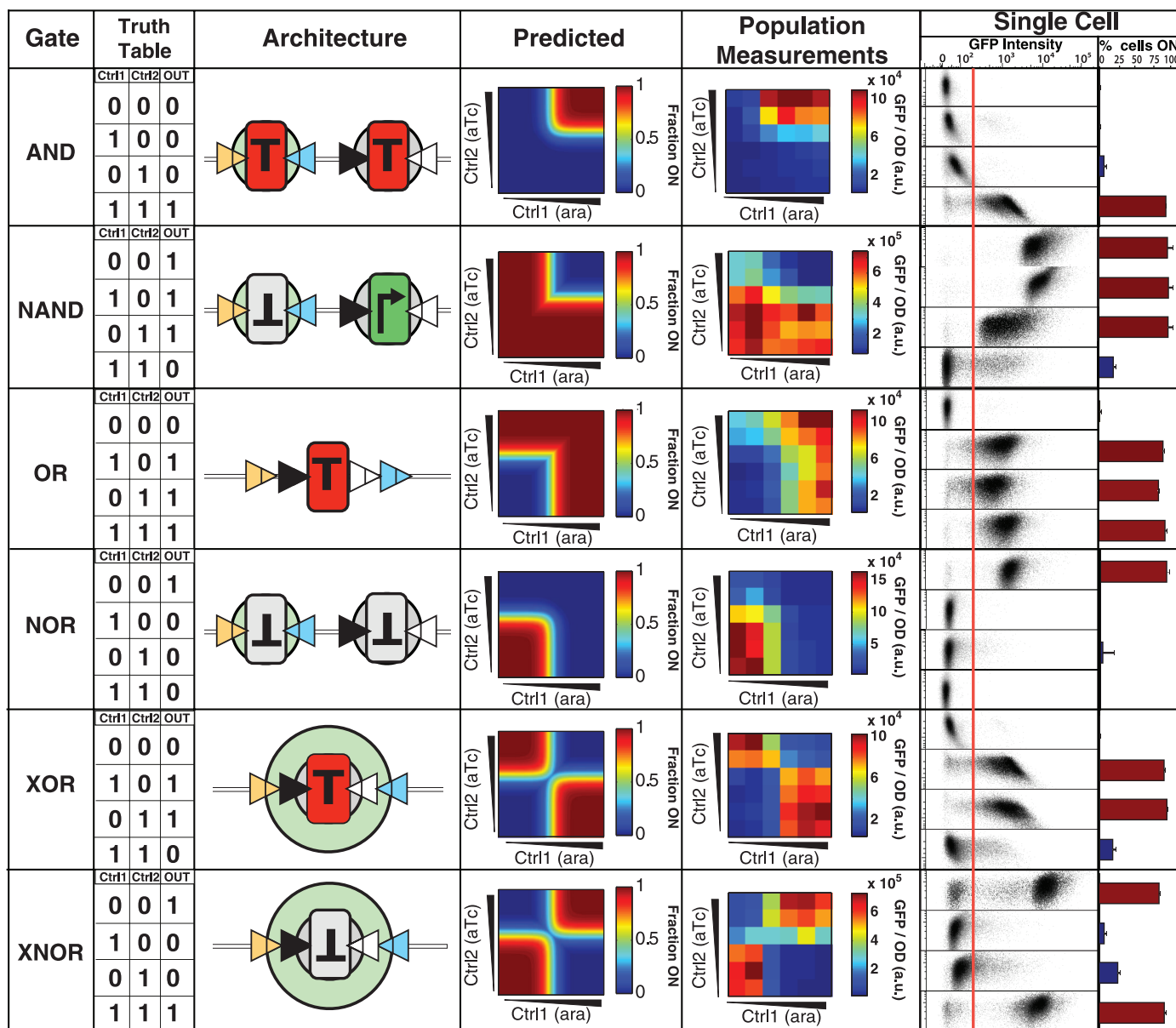


Fig. 2. Predicted and observed logic-gate performance plus digital-output thresholding. (Gate) Boolean logic functions. (Truth Table) Logical relationships between control (Ctrl) signals and output. (Architecture) Transcription element configurations for use in permanent Boolean integrase logic gates, including a constitutive promoter (NAND, green rightward arrow). (Predicted) Expected fraction of cells containing gates in a high-output state (heat map) calculated as described (23). (Population Measurements) Gate outputs assayed via plate reader for bulk cultures (23). Inducer concentrations

are 0, 0.02, 0.2, 2, 20, and 200 ng/ml for aTc and 0, 0.0001, 0.001, 0.01, 0.1, and 1% weight/volume (w/v) for ara. (Single Cell, GFP Intensity) Distribution of gate outputs [x axis GFP output measured in arbitrary units (a.u.); y axis side scatter] among single cells responding to control signals, as per gate-specific truth tables. A common output threshold segregates low/high outputs across all gates (vertical red line). Inducer concentrations are 200 ng/ml for aTc and 1% w/v for ara. (% Cells On) Fraction of cells encoding high outputs when scored by using a common output threshold.

Fig. 3. Digitization of control signals. (A) Distribution of XOR outputs among single cells (red contours) responding to an increasing control signal (blue contours). Each contour interval encompasses 5% of all cells; thick contours surround 50% of the total population. y axis, GFP output measured in arbitrary units (a.u.); x axis, side scatter at noted inducer concentrations. (B) As in (A) but for the second control signal. (C) Gate switching and digitization errors across an intermediate control signal change (0.2 to 2 ng/ml aTc, left/right of each frame). Gate-specific digitization thresholds (horizontal bars) were optimized and used to quantify fractions of false high cells given a low control signal and vice versa. Numbers within frames are high-given-low and low-given-high error rates. Numbers above boxes are combined error rates with standard deviation from three independent experiments. (D) As in (C), but in response to an intermediate change in the second control signal (1×10^{-4} to 0.5×10^{-2} ara, left/right of each frame).

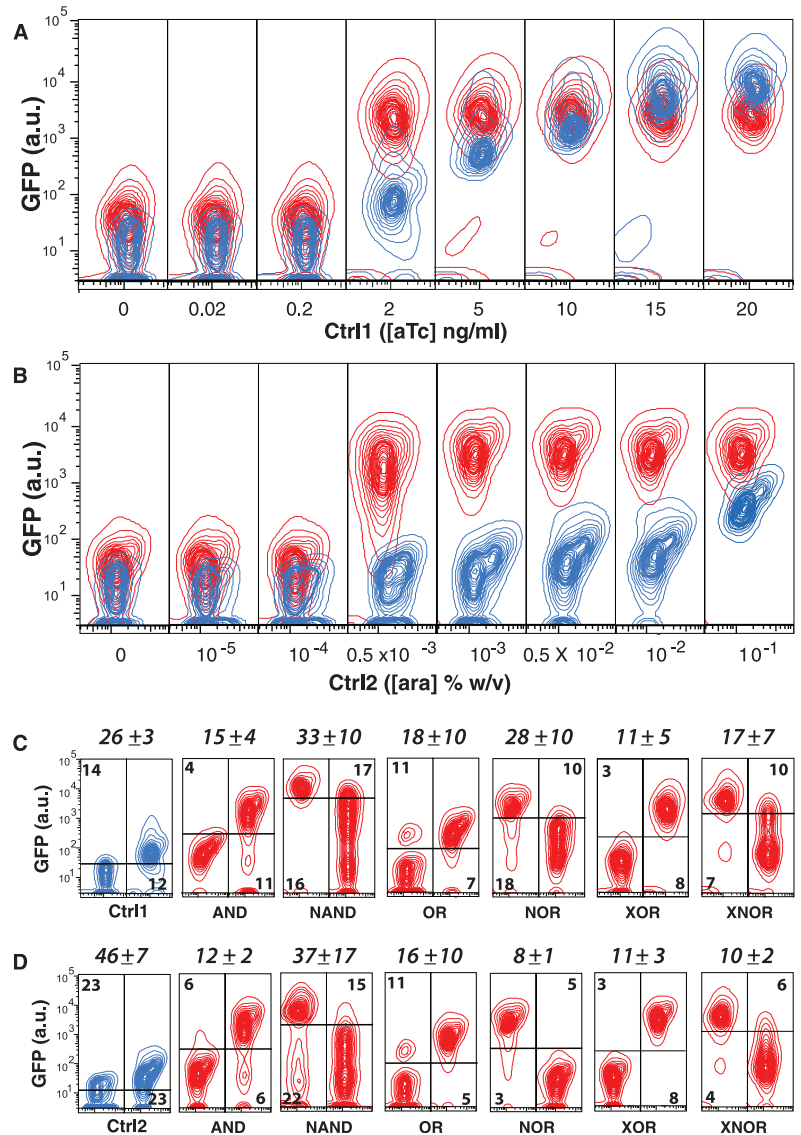
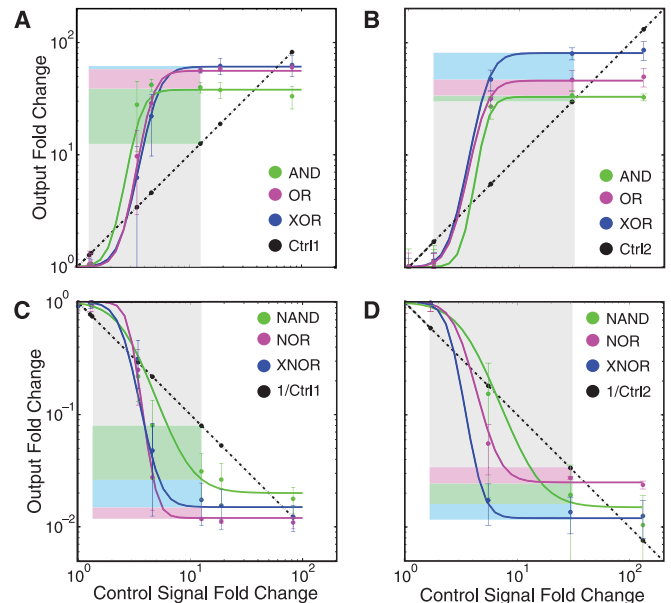


Fig. 4. Gain and amplification across common control signal ranges. Population-average response of amplifier gates to (A) increasing ara-mediated expression of TP901-1 integrase and (B) increasing aTc-mediated expression of Bxb1 integrase. Changes in output GFP levels produced by gates (colored lines) are directly compared to changes in control signals required for gate switching (increasing straight dashed lines). The response of each control signal to itself (gray boxes) is shown to highlight gate-specific amplification of control signals (colored boxes). (C and D) Responses of inverting amplifier gates. As in (A) and (B), except that fold changes for control signals are inverted (decreasing straight dashed lines) (figs. S8 and S10). Error bars indicate SD across three independent experiments.



systems by seamless integration of transcription logic elements within natural operons). Also, by separating gate inputs from gate control signals and by using a strong input signal modulated by an efficient asymmetric terminator, we were able to demonstrate and quantify signal amplification for all gates (Figs. 3 and 4).

Output signal levels vary within and among the gates reported here (Figs. 2 and 3 and figs. S9 and S10), although not more so than existing genetic logic. We believe that most variation arises from differences in RNA secondary structures well known to influence mRNA stability and translation initiation rates (fig. S15); such variation might be eliminated by using recently reported mRNA processing methods (24, 27). Further work is also required to realize precise level matching across all gates, and directed evolution of increasingly asymmetric terminators may be needed to reduce low output levels for most gates (fig. S10); additional gate-specific tuning of NAND would be required given its noncanonical logic element. Nevertheless, existing gates already support single-layer programmable digital logic, control-signal amplification, sequential logic, and cell-cell communication of intermediate logic states. Multi-input gates supporting high “fan-in” could be realized by using additional integrases (28) (fig. S16). Transcription-based gates can also likely be directly combined with other logic families to expand the power of engineered genetic computers. All logic gates and uses thereof demonstrated or disclosed here have been contributed to the public domain via the BioBrick Public Agreement (29).

References and Notes

1. B. Wang, M. Buck, *Trends Microbiol.* **20**, 376 (2012).
2. Y. Benenson, *Nat. Rev. Genet.* **13**, 455 (2012).
3. T. Miyamoto, S. Razavi, R. DeRose, T. Inoue, *ACS Synth. Biol.* **2**, 72 (2013).
4. D. R. Burrill, P. A. Silver, *Cell* **140**, 13 (2010).
5. J. Bonnet, P. Subsoontorn, D. Endy, *Proc. Natl. Acad. Sci. U.S.A.* **109**, 8884 (2012).
6. S. Basu, Y. Gerchman, C. H. Collins, F. H. Arnold, R. Weiss, *Nature* **434**, 1130 (2005).
7. M. E. Ortiz, D. Endy, *J. Biol. Eng.* **6**, 16 (2012).
8. Y. Y. Chen, M. C. Jensen, C. D. Smolke, *Proc. Natl. Acad. Sci. U.S.A.* **107**, 8531 (2010).
9. Z. Xie, L. Wroblewska, L. Prochazka, R. Weiss, Y. Benenson, *Science* **333**, 1307 (2011).
10. A. Tamsir, J. J. Tabor, C. A. Voigt, *Nature* **469**, 212 (2011).
11. T. S. Moon, C. Lou, A. Tamsir, B. C. Stanton, C. A. Voigt, *Nature* **491**, 249 (2012).
12. S. Ausländer, D. Ausländer, M. Müller, M. Wieland, M. Fussenegger, *Nature* **487**, 123 (2012).
13. For example, converting a NOR gate repressed by transcription factors to an OR gate activated by transcription factors requires changing how proteins interact with RNA polymerase (from competitive binding and occlusion to recruitment and initiation) and simultaneous reworking of the basal activity for core promoter elements (from a constitutively active promoter that can be repressed to a weak promoter that does not spontaneously initiate transcription yet that transcription factors activate).
14. C. Wadey, I. Deese, D. Endy, “Common signal carriers,” in *Adventures in Synthetic Biology* (OpenWetWare and Nature Publishing Group New York, 2005), chap. 3; available online at <http://hdl.handle.net/1721.1/46337>.
15. T. S. Ham, S. K. Lee, J. D. Keasling, A. P. Arkin, *PLoS ONE* **3**, e2815 (2008).
16. A. E. Friedland *et al.*, *Science* **324**, 1199 (2009).
17. P. A. Varadarajan, D. Del Vecchio, *IEEE Trans. Nanobioscience* **8**, 281 (2009).
18. J. Bardeen, W. Brattain, *Phys. Rev.* **74**, 230 (1948).
19. With transistor-based logic, gates use a base, emitter, and collector architecture that classically only allows for control of electrical current at one point on a wire by a single signal. Transcription-based logic allows RNA polymerase flow at a single point on DNA to be controlled, in theory, by as many independent recombinases as needed.
20. J. A. Lewis, G. F. Hatfull, *Nucleic Acids Res.* **29**, 2205 (2001).
21. W. R. A. Brown, N. C. O. Lee, Z. Xu, M. C. M. Smith, *Methods* **53**, 372 (2011).
22. B. Cantan, A. Labno, D. Endy, *Nat. Biotechnol.* **26**, 787 (2008).
23. Materials and methods are available as supplementary materials on *Science* Online.
24. C. Lou, B. Stanton, Y.-J. Chen, B. Munsky, C. A. Voigt, *Nat. Biotechnol.* **30**, 1137 (2012).
25. L. Pasotti, N. Politi, S. Zucca, M. G. Cusella De Angelis, P. Magni, *PLoS ONE* **7**, e39407 (2012).
26. P. Siuti, J. Yazbek, T. K. Lu, *Nat. Biotechnol.* (2013).
27. L. Qi, R. E. Haurwitz, W. Shao, J. A. Doudna, A. P. Arkin, *Nat. Biotechnol.* **30**, 1002 (2012).
28. G. F. Hatfull *et al.*, *J. Virol.* **86**, 2382 (2012).
29. <https://biobricks.org/bpa/>

Acknowledgments: We thank M. Juul, T. Knight, S. Kushner, C. Smolke, B. Townshend, the Endy and Smolke labs, and the Stanford Shared FACS Facility. Funding was provided by the NSF Synthetic Biology Engineering Research Center, Stanford Center for Longevity, Stanford Bio-X, the Townshend/Lamarre Family Foundation, and the Siebel Foundation. DNA sequences are available in GenBank (accession nos. KC529324 to KC529332). DNA constructs will be made available via Addgene.

Supplementary Materials

www.sciencemag.org/cgi/content/full/science.1232758/DC1
Materials and Methods
Figs. S1 to S15
Appendices S1 to S4
References (30–44)
Movie S1

14 November 2012; accepted 13 March 2013
Published online 28 March 2013;
10.1126/science.1232758

Controlled Flight of a Biologically Inspired, Insect-Scale Robot

Kevin Y. Ma,^{†*} Pakpong Chirattananon,[†] Sawyer B. Fuller, Robert J. Wood

Flies are among the most agile flying creatures on Earth. To mimic this aerial prowess in a similarly sized robot requires tiny, high-efficiency mechanical components that pose miniaturization challenges governed by force-scaling laws, suggesting unconventional solutions for propulsion, actuation, and manufacturing. To this end, we developed high-power-density piezoelectric flight muscles and a manufacturing methodology capable of rapidly prototyping articulated, flexure-based sub-millimeter mechanisms. We built an 80-milligram, insect-scale, flapping-wing robot modeled loosely on the morphology of flies. Using a modular approach to flight control that relies on limited information about the robot's dynamics, we demonstrated tethered but unconstrained stable hovering and basic controlled flight maneuvers. The result validates a sufficient suite of innovations for achieving artificial, insect-like flight.

Using flapping wings and tiny nervous systems, flying insects are able to perform sophisticated aerodynamic feats such as deftly avoiding a striking hand or landing on flowers buffeted by wind. How they perform these

feats—from sensorimotor transduction to the unsteady aerodynamics of their wing motions—is just beginning to be understood (1–3), aided in part by simulation (4) and scaled models (5). Motivated by a desire for tiny flying robots with comparable maneuverability, we seek to create a robotic vehicle that mirrors these basic flight mechanics of flies. At the scale of flies, no such vehicle has been demonstrated to date because of the severe miniaturization challenges that must be overcome for an insect-sized device (6). Con-

ventional technologies for macroscale aircraft propulsion and manufacturing are not viable for millimeter-scale robots because of inefficiencies that arise from force scaling, suggesting a biologically inspired solution based on flapping wings (7–9). Here, we report an aggregation of innovations in design, manufacturing, actuation, and control to create an insect-scale flying robot—a robotic fly—that successfully demonstrates tethered but unconstrained flight behavior reminiscent of flying insects.

For inspiration of form and function, we used *Diptera* (flies) as a model system because of the relative simplicity of the flight apparatus—flies by classification have only two wings—and the exemplary aerial agility that they exhibit. Dipteran flight has been well-studied (5, 10–18), and it is understood that insect wings undergo a complex trajectory defined by three rotational degrees of freedom (10). This has been simplified in the robotic fly to a reciprocating flapping motion in which the wings' pitch rotation is regulated with passive compliant flexures (19)—an enabling simplification for mechanism design and manufacture. Key aspects of the oscillatory wing motion are the flapping frequency and wing stroke amplitude; the robotic fly achieves 120 Hz and 110°, respectively, similar to the 130-Hz wing beat

School of Engineering and Applied Sciences and the Wyss Institute for Biologically Inspired Engineering, Harvard University, Cambridge, MA 02138, USA.

*Corresponding author. E-mail: kevinma@seas.harvard.edu
[†]These authors contributed equally to this work.